Nonlinear Control of Mechanical Systems with one Degree of Underactuation

C. Chevallereau*, J.W. Grizzle† and C.H. Moog*
*IRCCyN, Ecole Centrale de Nantes, UMR CNRS 6597
BP 92101, 1 rue de la Noë, 44321 Nantes cedex 03, France
Email: Christine.Chevallereau,Claude.Moog@irccyn.ec-nantes.fr
†Department of Electrical Engineering and Computer Science
The University of Michigan, Ann Arbor, MI, 48109-2122, USA
Email:grizzle@umich.edu

***Abstract*— Numerous robotic tasks associated with underactuation have been studied in the literature. For a large number of these in the plane, the mechanical models have a cyclic variable, the cyclic variable is unactuated, and all shape variables are independently actuated. This paper formulates and solves two control problems for this class of models. If the generalized momentum conjugate to the cyclic variable is conserved, a set of flat outputs is defined. If the generalized momentum conjugate to the cyclic variable is not conserved, a feedback that asymptotically stabilizes an equilibrium is given. The results are illustrated on a ballistic flip motion and on a balancing task.**

I. Introduction

Underactuated mechanical systems have fewer actuators than degrees of freedom. Underactuation is naturally associated with dexterity. For example, the act of standing with one foot flat on the ground is not viewed as particulary dexterous, whereas a headstand or *sur les pointes* (ballet) are considered dexterous. In headstands or when on *pointe*, the contact point between the body and ground is acting as a pivot without actuation. These are underactuated systems. In these examples, a typical control task would be to hold an equilibrium pose with stability, or to execute a motion (e.g., a *relevé lent*, *battement*) without falling over (i.e., with internally bounded states). Motions that include a ballistic phase are also often viewed as dexterous. Examples include dismounting from a highbar or platform diving. In these cases, the underactuation is manifest in the lack of contact with any surface. The ballistic phase is normally of short duration since reestablishing contact with a surface (e.g., ground, mat, water, ...) is an objective of the maneuver. A typical control problem would be to execute a predefined motion, with emphasis on achieving a final state that is compatible with an elegant landing.

The literature on underactuated systems and nonholonomic systems is vast. A few representative control works include the study of accessibility in [11], stabilization of equilibria through passivity techniques in [15], stabilization and tracking via backstepping in [20], and path planning in [1]. The planar mechanical systems studied here are motivated in Section II. The class of systems includes the Acrobot [21], [14], the brachiating robot of [13], the gymnast robots of [12], [23] when pivoting on a highbar or when dismounting from the highbar, the stance and flight phase models of Raibert's one-legged hopper [16] as well as RABBIT [4], [3], and the ballistic phase of the 4-link planar robot in [19]. Though some are attached to a frictionless pivot and others are undergoing ballistic motion, these systems have in common the existence of an unactuated cyclic variable [7]. Their models are described in a form convenient for analysis in Section III. The key to solving certain control problems associated with these underactuated systems is the construction of a special scalar function of the configuration variables that has at least relative three with respect to one of the control inputs after an appropriate state variable feedback. Section IV uses this function to determine a set of flat outputs for systems where the generalized momentum conjugate to the cyclic variable is conserved. The result is illustrated on a ballistic flip motion for a two-link robot. Section V uses this special function to propose a constructive procedure for stabilizing an equilibrium point for systems where the generalized momentum conjugate to the cyclic variable is not conserved. The result is illustrated on a balancing task for a three-link robot. A more complete version of these results has been submitted for publication in [9].

II. The Studied Systems

Two classes of systems are considered. The first class consists of $N \geq 2$ planar rigid bodies connected in a tree structure with the base attached to an inertial reference frame via a pivot, that is, an unactuated revolute joint. It is supposed that each connection of two links is independently actuated so that the system has one degree of underactuation (N degrees of freedom with $N-1$ independent actuators). It is further supposed that the pivot is frictionless. Figure 1a shows an example of such a system along with the indicated coordinates, $q = (q_0,\ q_1,\ \cdots,\ q_{N-1})$. The kinetic energy is quadratic, $K = \frac{1}{2}\dot{q}^T D(q)\dot{q}$, with D positive definite. Since the kinetic energy is independent of the orientation of the reference frame, D is independent of q_0; that is $\frac{\partial D(q)}{\partial q_0} \equiv 0$. The coordinate q_0 is said to be cyclic [7]. The potential energy depends only on the configuration variables. Denote the Lagrangian by $L = K - V$,

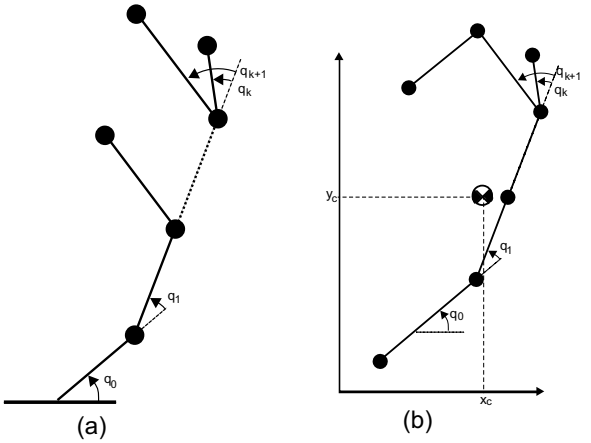

Fig. 1. Two planar tree structures: one is attached to an inertial frame via a freely acting pivot, one evolves in ballistic motion. All joints between two links are actuated. A coordinate convention is indicated.

then the dynamic model is:

$$\frac{d}{dt}\frac{\partial L}{\partial \dot{q}_k} - \frac{\partial L}{\partial q_k} = \begin{cases} 0 & k = 0 \\ \Gamma_k & k = 1, \cdots, N-1 \end{cases}, \quad (1)$$

where Γ_k is the torque applied on joint k. The model thus takes the form

$$D(q)\ddot{q} + C(q,\dot{q})\dot{q} + G(q) = \begin{bmatrix} 0 \\ \Gamma \end{bmatrix}. \quad (2)$$

The second class of systems consists of $N \geq 2$ planar rigid bodies, once again connected in a tree structure (each connection of two links is independently actuated), but this time, it is assumed that the mechanism is undergoing ballistic motion. Such a system has three degrees of underactuation: $N+2$ degrees of freedom and $N-1$ independent actuators. Figure 1b shows an example of such a system along with the indicated coordinates, $q_e = (q, x_c, y_c)$. In these coordinates the dynamics of the body coordinates, q, and the Cartesian coordinates of the center of mass, (x_c, y_c), are decoupled

$$\begin{array}{rcl} \bar{D}(q)\ddot{q} + \bar{C}(q,\dot{q})\dot{q} + \bar{G}(q) & = & \begin{bmatrix} 0 \\ \Gamma \end{bmatrix} \\ \ddot{x}_c & = & 0 \\ \ddot{y}_c & = & g_0, \end{array} \quad (3)$$

where in a vertical plane g_0 is the gravitational constant. Since the center of mass coordinates are unactuated, the control of the system (3) can be reduced to the control of a system having one degree of underactuation as in (2) by eliminating the trivial dynamics $\ddot{x}_c = 0$, $\ddot{y}_c = g_0$. The next section presents the model in a form that is convenient for analysis.

III. The Model Form

With $N-1$ actuators, it is possible to freely set the acceleration of the $N-1$ actuated variables. Let $F(q,\dot{q}) := C(q,\dot{q})\dot{q} + G$ and partition the generalized coordinates into actuated and unactuated parts per $q = (q_0, \bar{q}_1)$, $\bar{q}_1 = (q_1, \cdots, q_{N-1})$. This induces a decomposition of the model (2)

$$\begin{array}{rcccccc} d_{0,0}\ddot{q}_0 & + & D_{0,1}\ddot{\bar{q}}_1 & + & F_0 & = & 0 \\ D_{1,0}\ddot{q}_0 & + & D_{1,1}\ddot{\bar{q}}_1 & + & F_1 & = & \Gamma. \end{array} \quad (4)$$

Define

$$\begin{array}{rcl} \bar{D} & = & D_{1,1} - D_{1,0}D_{0,1}/d_{0,0} \\ \bar{F} & = & F_1 - D_{1,0}F_0/d_{0,0} \end{array} \quad (5)$$

where $d_{0,0}$ is never zero because D is positive definite. If the torques are chosen such that

$$\Gamma = \bar{D}v + \bar{F}, \quad (6)$$

then the last $N-1$ rows of the dynamic model become

$$\ddot{q}_j = v_j \quad j = 1, \cdots, N-1. \quad (7)$$

Because q_0 is a cyclic variable, $\frac{\partial K}{\partial q_0} = 0$, the first line of the dynamic model defined in (1) becomes

$$\dot{\sigma} = -\frac{\partial V}{\partial q_0}(q), \quad (8)$$

where $\sigma = \frac{\partial L}{\partial \dot{q}_0}$. Because the kinetic energy is quadratic, and potential energy does not depend on joint velocities, $\frac{\partial V}{\partial \dot{q}_0} = 0$, it follows that

$$\sigma = \sum_{k=0}^{N-1} d_{0,k}(q_1, \cdots, q_{N-1})\dot{q}_k, \quad (9)$$

where $d_{0,k}$, $k = 0, \cdots, N-1$ are the entries in the first row of D. In the case of a mechanical system corresponding to Figure 1a, because the reference frame has been attached at the pivot point, σ is in fact the angular momentum about the pivot point. In the case of a system corresponding to Figure 1b, σ is the angular momentum about the center of mass. Because $d_{0,0}$ is never zero, (9) can be used to solve for the angular velocity of the cyclic variable in terms of σ. The dynamic model of the robot can thus be expressed in the form

$$\begin{array}{rcl} \dot{q}_0 & = & \frac{\sigma}{d_{0,0}(q_1,\cdots,q_{N-1})} - \sum_{k=1}^{N-1} \frac{d_{0,k}}{d_{0,0}}(q_1, \cdots, q_{N-1})\dot{q}_k \\ \dot{\sigma} & = & -\frac{\partial V}{\partial q_0}(q) \\ \ddot{q}_j & = & v_j \quad j = 1, \cdots, N-1. \end{array} \quad (10)$$

IV. Systems where the generalized momentum conjugate to the cyclic variable is conserved

If the conjugate momentum is conserved, the equation $\dot{\sigma} = 0$ yields a nonholonomic constraint, which significantly complicates trajectory generation and control of the system [11], [19]. In particular, the motion of the system is restricted to a lower dimensional surface that is fixed by the initial conditions, and thus, whenever possible, motion planning should be done on-line. In the following a set of outputs is developed that leads to exact linearization of the controllable subsystem. Such outputs are said to be flat outputs [18], [5]; they can be used to simplify motion planning [18].

A. Mechanical structure with 2 links

Consider first a mechanical structure consisting of only two links:

$$\begin{array}{rcl} \dot{q}_0 & = & \frac{\sigma}{d_{0,0}(q_1)} - \frac{d_{0,1}}{d_{0,0}}(q_1)\dot{q}_1 \\ \ddot{q}_1 & = & v_1. \end{array} \quad (11)$$

When momentum is conserved, it is well known that the only way to act on the rotational speed of the body about the

center of mass is to modify the inertia. This fact is not directly evident when the equations are expressed in the form (11). For an articulated two body system, this fact can be easily seen if the angular momentum is rewritten in terms of only one rotational velocity

$$\sigma = d_{0,0}(q_1)\dot{q}_0 + d_{0,1}(q_1)\dot{q}_1 = d_{0,0}(q_1)\dot{p}_1 \tag{12}$$

where

$$\dot{p}_1 = \dot{q}_0 + \frac{d_{0,1}}{d_{0,0}}(q_1)\dot{q}_1, \tag{13}$$

and $d_{0,0}(q_1)$ is the inertia of the mechanism about the pivot point. The "global orientation" associated with this velocity is

$$p_1 = q_0 - q_0^* + \int_{q_1^*}^{q_1} \frac{d_{0,1}}{d_{0,0}}(\tau)d\tau. \tag{14}$$

The integral in (14) is well-defined because the integrand is smooth and the integral is evaluated over a closed and bounded interval. The same function has appeared in [14] in a different context. An explicit formula for p_1 will be given shortly in the worked example.

Since the control v_1 acts on the acceleration, $\ddot{q}_1$, it only acts on the jerk of p_1. Choosing p_1 as an output, ($y_1 = p_1$) yields

$$p_1^{(3)} = -\frac{\sigma \frac{d(d_{0,0})}{dq_1}}{d_{0,0}^2}v_1 - \frac{\sigma(d_{0,0}\frac{d^2(d_{0,0})}{dq_1^2} - 2(\frac{d(d_{0,0})}{dq_1})^2)}{d_{0,0}^3}\dot{q}_1^2. \tag{15}$$

If $\sigma \frac{d(d_{0,0})}{dq_1}$ is non-zero, one can use feedback to define a new control w_1 by

$$v_1 = (\frac{\sigma \frac{d(d_{0,0}))}{dq_1}}{d_{0,0}^2})^{-1}(w_1 + \frac{\sigma(d_{0,0}\frac{d^2(d_{0,0})}{dq_1^2} + 2(\frac{d(d_{0,0})}{dq_1})^2)}{d_{0,0}^3}\dot{q}_1^2), \tag{16}$$

after which the model of the two-link robot becomes linear

$$p_1^{(3)} = w_1. \tag{17}$$

In other words, p_1 is a flat output [18], [5] and the model (11) can be exactly linearized with the new state variables p_1, $\dot{p}_1$, $\ddot{p}_1$ and the feedback (15). An example based on [6] is given next.

B. Example: Planar Two link Structure in Ballistic Motion

1) Mathematical representation: The control objective will be to effect a motion with boundary constraints that are motivated by bipedal running [4]. The mechanism consists of three point masses joined by two massless bars in an actuated, revolute joint. The point masses are given by $m_0 = 1$, $m_1 = 2$, $m_2 = 1$; the bar connecting m_0 to m_1 has length $L_1 = 1$ and that connecting m_1 to m_2 has length $L_2 = 1$. The complete dynamic model is easily obtained using the method of Lagrange and yields immediately

$$\begin{array}{rcl} \dot{q}_0 &=& \frac{\sigma}{d_{0,0}(q_1)} - \frac{d_{0,1}}{d_{0,0}}(q_1)\dot{q}_1 \\ \dot{\sigma} &=& 0 \\ \ddot{q}_1 &=& v \\ \ddot{x}_c &=& 0 \\ \ddot{y}_c &=& g_0, \end{array} \tag{18}$$

with control v and

$$\begin{array}{rcl} d_{0,0}(q_1) &=& a_{00} + a_{01}cos(q_1) \\ d_{0,1}(q_1) &=& a_{10} + a_{11}cos(q_1) \\ a_{00} &=& \frac{m_0(m_1+m_2)L_1^2 + m_2(m_0+m_1)L_2^2}{m_0+m_1+m_2} \\ a_{01} &=& 2a_{11} \\ a_{10} &=& \frac{m_2(m_0+m_1)L_2^2}{m_0+m_1+m_2} \\ a_{11} &=& \frac{m_0 m_2 L_1 L_2}{m_0+m_1+m_2}. \end{array} \tag{19}$$

The strongly accessible portion of the model has dimension three, and involves $q_0, q_1, \dot{q}_1$. Due to ballistic motion, there is a five dimensional uncontrollable subsystem given by $x_c, y_c, \dot{x}_c, \dot{y}_c, \sigma$. How these two parts interact in a path planning problem is explained next.

2) Interaction through boundary conditions: The flight phases of a gymnastic robot, such as a tumbler or a bipedal runner, are typically short-term motions that alternate with single support phases. The creation of an overall satisfactory motion is closely tied to achieving correct boundary conditions at the interfaces of the flight and single support phases. The state of the robot at the end of a flight phase is typically more important than the exact trajectory followed during the flight phase. At the beginning and end of a flight phase, the robot is in contact with a surface (assumed here to be identified with the horizontal component of the world frame). There are two holonomic constraints that tie the position and velocity of the center of mass to those of the angular coordinates. Conservation of angular momentum through $\dot{\sigma} = 0$ yields an additional (nonholonomic) constraint on the angular velocities. In particular, the desired final joint velocities must be chosen to satisfy this constraint. The duration of the flight phase, T, is determined from $\ddot{y}_c = g_0$, with the initial conditions coming from the initial positions and velocities of the angular coordinates at lift-off, and the end condition of the height of the center of mass coming from the desired final configuration of the angular coordinates at touch-down.

3) Determining a ballistic motion trajectory in linearizing coordinates: The new coordinates are constructed from p_1 and its first two derivatives. Define p_1 by (14). Direct computation leads to

$$p_1 = q_0 + \frac{a_{11}}{a_{01}}q_1 + 2A\arctan\left(\frac{a_{00}-a_{01}}{\sqrt{a_{00}^2 - a_{01}^2}}\tan(\frac{q_1}{2})\right) \tag{20}$$

where $A = \frac{a_{10}}{\sqrt{a_{00}^2-a_{01}^2}} - \frac{a_{00}a_{11}}{a_{01}\sqrt{a_{00}^2-a_{01}^2}}$

$$\dot{p}_1 = \frac{\sigma}{a_{00} + a_{01}\cos(q_1)} \tag{21}$$

$$\ddot{p}_1 = \frac{\sigma a_{01}\sin(q_1)}{(a_{00} + a_{01}\cos(q_1))^2}\dot{q}_1 \tag{22}$$

To determine the linearizing control, one more derivative is needed

$$p_1^{(3)} = \sigma a_{01}\frac{(2a_{01} + a_{00}\cos(q_1) - a_{01}\cos^2(q_1))}{(a_{00} + a_{01}\cos(q_1))^3}\dot{q}_1^2 + M_{1,1}v \tag{23}$$

where $M_{1,1} = \frac{\sigma a_{01}\sin(q_1)}{(a_{00}+a_{01}\cos(q_1))^2}$. Wherever $M_{1,1} \neq 0$, a linearizing feedback can be constructed such that

$$p_1^{(3)} = w. \tag{24}$$

For arbitrary initial and final conditions of the linear model (24), it is trivial to define a feasible trajectory. Indeed, it suffices to define a three-times continuously differentiable function passing from given initial values to given final values. One could even use a polynomial of order five or greater for $p_1(t)$.

Since the change of coordinates going from (11) to (24) is local, not every solution of (24) can be mapped back onto a solution of (11). From (21), since σ is constant and since $d_{0,0}$ is bounded, so is $\dot{p}_1$. These kinds of constraints, which must be applied point-wise in time on the trajectories of (24), are made explicit by computing the inverse of the coordinate change.

4) Constraints point-wise in time associated with the linearizing coordinates: The calculation of $q_0, q_1, \dot{q}_1$ in terms of $p_1, \dot{p}_1, \ddot{p}_1$ yields

$$\begin{aligned} q_1 &= \arccos\left(\frac{\frac{\sigma}{\dot{p}_1} - a_{00}}{a_{01}}\right) \\ q_0 &= p_1 - \frac{a_{11}}{a_{01}} q_1 - 2A \arctan\left(\frac{a_{00} - a_{11}}{\sqrt{a_{00}^2 - a_{01}^2}} \tan\left(\frac{q_1}{2}\right)\right) \\ \dot{q}_1 &= \frac{\ddot{p}_1 (a_{00} + a_{01}\cos(q_1))^2}{\sigma a_{01} \sin(q_1)} \end{aligned} \tag{25}$$

The first equation only admits a solution for $\frac{\sigma}{a_{00}-a_{01}} \leq \dot{p}_1 \leq \frac{\sigma}{a_{00}+a_{01}}$, and then has two solutions: one for $0 \leq q_1 < \pi$ and another for $-\pi \leq q_1 < 0$. These two domains for the cosine define two "configuration classes" of the robot, with the extreme points of the domains corresponding to the links being completely folded or unfolded. The sign of $\dot{q}_1$ is determined by continuity (with torque control, there cannot be discontinuities in the velocity). At the extreme points of the domains, $\dot{p}_1$ attains an extremum and consequently, $\ddot{p}_1$ is zero. The robot will then pass through the singularity, and change configuration classes. Consequently, when generating a motion, two cases can present themselves, according to whether the motion stays always in the same configuration class or not. In this paper, the study is limited to motion with the initial and final configuration in the same configuration class, then a trajectory can be generated by imposing $\frac{\sigma}{a_{00}-a_{01}} < \dot{p}_1(t) < \frac{\sigma}{a_{00}+a_{01}}$. Both open-loop and feedback controls are equally easily computed starting from the linear model. A more complete treatment is given in [9].

For this simulation, the mass m_0 of the robot is supposed initially in contact with the ground, with configuration defined by $q_0 = 3\pi/4, q_1 = -\pi/4$, and angular velocities $\dot{q}_0 = -5, \dot{q}_1 = 0$. The objective is to transfer the robot at the end of a flight phase so that when the mass m_2 of the robot touches the ground, its configuration is $q_0 = -0.5, q_1 = -\pi/4$ with angular velocity proportional to $\dot{q}_0 = 1, \dot{q}_1 = 0$. The initial and final configurations are depicted in Figure (2); they belong to the same configuration class. From the initial conditions of the robot and the desired final configuration, the flight time is computed as $T = 0.5173$. Conservation of angular momentum implies that $\dot{q}_0(T) = -5$.

The initial and final values of p_1 and its first two derivatives were computed from (20), (21), and (22). A fifth-order polynomial of t was defined that satisfied these boundary conditions.

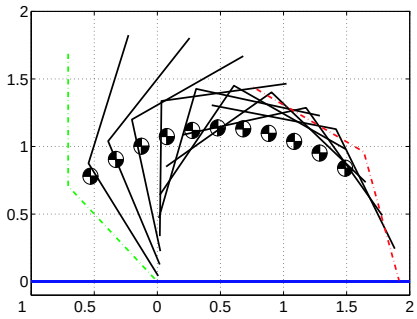

Fig. 2. The motion of the robot passes from left to right without passing through a singularity. The initial and final configurations ($\cdot - \cdot - \cdot$) belong to the same configuration class. The center of gravity follows a parabolic trajectory.

The resulting trajectories of $p_1, \dot{p}_1, \ddot{p}_1$ are depicted in Figure 3; the point-wise in time constraints associated with (25) are met. The input torque Γ for the system was computed using (23) and (6). The resulting trajectories in terms of q and $\dot{q}$ are shown in Figure 4 and the evolution of the robot in the vertical plane is presented in Figure 2. An animation of the motion is available at [8].

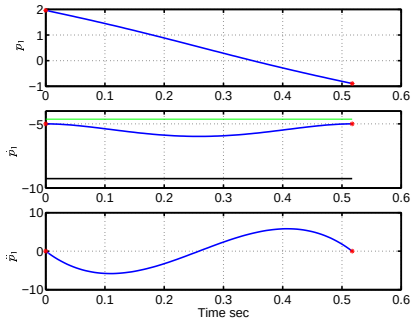

Fig. 3. Based on the initial and final conditions of the flight phase, a trajectory for p_1 and its derivatives is derived. The plot shows that $\dot{p}$ satisfies the constraint $\frac{\sigma}{a_{00}-a_{01}} \leq \dot{p}_1(t) \leq \frac{\sigma}{a_{00}+a_{01}}$

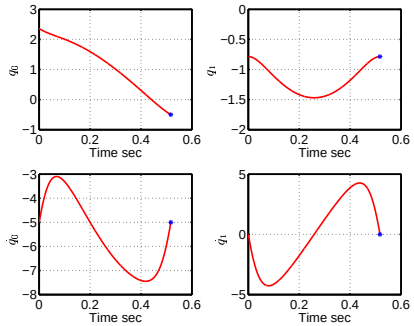

Fig. 4. The computed open-loop control transfers the robot from its initial state to the desired final state (shown with * on the graphics).

C. Mechanical structure with N links

The above results can be extended to N-link mechanisms, though a dynamic feedback is needed to linearize the model.

The complete result form [9] is only sketched here. To define $N-1$ flat outputs, $N-2$ of the $N-1$ actuated variables are used, and the last output component is constructed along the lines of the case of a 2-link mechanism. The generalized momentum is first expressed as

$$\sigma = d_{0,0}(q_1, \cdots, q_{N-1}) \left(\dot{q}_0 + \sum_{k=1}^{N-1} \frac{d_{0,k}}{d_{0,0}}(q_1, \cdots, q_{N-1}) \dot{q}_k \right). \tag{26}$$

Regrouping terms in $\dot{q}_0$ and $\dot{q}_1$, σ is rewritten in the form

$$\sigma = d_{0,0}(q_1, \cdots, q_{N-1}) \left(\dot{p}_1 - \sum_{k=2}^{N-1} \beta_k(q_1, \cdots, q_{N-1}) \dot{q}_k \right) \tag{27}$$

where

$$p_1 = q_0 - q_0^* + \int_{q_1^*}^{q_1} \frac{d_{0,1}}{d_{0,0}}(\tau, q_2, \cdots, q_{N-1}) d\tau, \tag{28}$$

$$\begin{aligned} \beta_k(q_1, \cdots, q_{N-1}) \quad = \quad & \int_{q_1^*}^{q_1} \frac{\partial}{\partial q_k} \frac{d_{0,1}}{d_{0,0}}(\tau, q_2, \cdots, q_{N-1}) d\tau \\ & - \frac{d_{0,k}}{d_{0,0}}(q_1, \cdots, q_{N-1}), \end{aligned} \tag{29}$$

and $\dot{p}_1$ is given by

$$\dot{p}_1 = \frac{\sigma}{d_{0,0}(q_1, \cdots, q_{N-1})} + \sum_{k=2}^{N-1} \beta_k(q_1, \cdots, q_{N-1}) \dot{q}_k. \tag{30}$$

Since $\dot{p}_1$ does not depend on $\dot{q}_1$, it must be differentiated at least twice more before v_1 appears. On the other hand, the calculation of $p_1^{(3)}$ involves $q_j^{(3)}$, and thus a dynamic extension is needed: $\dot{v}_i = \mu_i, i = 2, \cdots, N-1$; also, rename $v_1 = \mu_1$. If the term in $p_1^{(3)}$ multiplying μ_1 is non-zero, a feedback can be defined to transform the system into $y_k^{(3)} = w_k,\ 1 \leq k \leq N-1$ (see Section V-B), and the methods presented for a 2-link robot can be applied to an N-link mechanism [9].

V. Systems where the generalized momentum conjugate to the cyclic variable is not conserved

If the conjugate momentum is not conserved, that is, $\frac{\partial V}{\partial q_0}(q) \neq 0$, the robot's motion is not constrained. Results presented in [9] indicate that, generally, this class of underactuated systems is not static feedback linearizable, and results presented in [17] show that generally there do not exist flat outputs depending only on the configuration variables (recall that such outputs were used in the previous case where conjugate momentum was conserved). Said another way, for this class of models, it is not known how to choose $N-1$ outputs that result in an empty zero dynamics (in fact, it is reasonable to conjecture that such outputs do not generally exist). Of course if N=2, the situation is clear - the system is not flat. A realistic goal however is seek a set outputs such that the associated zero dynamics is one dimensional and exponentially stable, which is the problem addressed here. The results are first discussed for a two-link robot and then sketched for an N-link robot. The result will be illustrated through stabilization and trajectory tracking on a three-link robot. The method used in this section can be seen as an extension of [14] for two-link robots and [2] for robots that have a star structure.

A. Mechanical structure with 2 links

Since it is a single input system, feedback linearizability (flatness) is fully characterized. A standard choice of outputs would be $y_1 = q_1 - q_1^e$, which has relative degree two. Such a choice leads to a two-dimensional zero dynamics and it can be shown that the zero dynamics can never have an asymptotically stable equilibrium [22]. By seeking an output component with a relative degree higher than two, the dimension of the zero dynamics can be reduced, opening up the possibility of creating one that is scalar and asymptotically stable. Using the previous analysis, two relative degree three functions available are the conjugate momentum, σ defined in (8), and p_1 defined in (14). Any function of p_1 and σ also has relative degree three and p_1 and σ are the only two independent functions with relative degree three. Since by (12), σ is proportional to $\dot{p}_1$ through the strictly positive quantity $d_{0,0}$, the choice of output

$$y_1 = K(p_1 - p_1^e) + \sigma, \tag{31}$$

where p_1^e is the value at an equilibrium point q^e, should yield the zero dynamics

$$\dot{p}_1 = -\frac{K}{d_{0,0}}(p_1 - p_1^e). \tag{32}$$

Since $d_{0,0}$ is positive, (32) is exponentially stable for all $K > 0$. The technical conditions under which all of this holds are clarified in [9]. The main point is that a feedback controller that drives the output (31) to zero exponentially fast will (locally) exponentially stabilize the system when conjugate momentum is not conserved.

B. Mechanical structure with N links

Let $(q^e, 0)$ be an equilibrium of the N-link mechanism (10). The construction of a set of outputs yielding a one-dimensional, exponentially stable zero dynamics involves augmenting the output (31) with the $(N-2)$ outputs $y_i = q_i - q_i^e$, for $i = 2, \cdots, N-1$, and with p_1 defined as in (28). Since the third derivative of y_1 depends on $q_i^{(3)}$, for $i = 2, \cdots, N-1$, a dynamic extension is defined:

$$\dot{v}_i = \mu_i, i = 2, \cdots, N-1, \tag{33}$$

along with the renaming of $v_1 = \mu_1$. Clearly, $y_k^{(3)} = \mu_k$, for $2 \leq k \leq N-1$. The third derivative of y_1 can be written as

$$y_1^{(3)} = f(q, \dot{q}, v_2, \ldots, v_{N-1}) + M_{1,1}(q, \dot{q})\mu_1 + \sum_{k=2}^{N-1} K\beta_k \mu_k \tag{34}$$

with

$$M_{1,1} = -K\frac{\sigma}{d_{0,0}^2}\frac{\partial d_{0,0}}{\partial q_1} + K\sum_{k=2}^{N-1}\left(\frac{\partial \beta_k}{\partial q_1}\dot{q}_k\right) - \frac{\partial^2 V}{\partial q_0^2}\frac{d_{0,1}}{d_{0,0}} - \frac{\partial^2 V}{\partial q_1 \partial q_0}.$$

Define a feedback controller in w by

$$\mu = \begin{bmatrix} M_{1,1} & K\beta_2 \cdots K\beta_{N-1} \\ 0 & I_{(N-2)\times(N-2)} \end{bmatrix}^{-1} \left[w - \begin{bmatrix} f \\ 0 \end{bmatrix} \right], \tag{35}$$

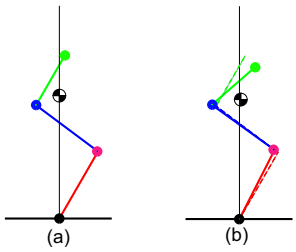

Fig. 5. Three-link mechanism, connected at a pivot. (a) shows an equilibrium pose (b) shows the initial condition used in the simulation.

yielding $y^{(3)} = w$. If $M_{1,1}$ is non-zero at the equilibrium point, the zero dynamics is locally well defined and is given by

$$\dot{p}_1 = -\frac{K}{d_{0,0}(q_1(p_1, q^e), q_2^e, \cdots, q_{N-1}^e)}(p_1 - p_1^e); \qquad (36)$$

the supporting details are given in [9]. From [10], it immediately follows that a feedback providing (local) asymptotic tracking with internally bounded states is

$$w = y_r^{(3)} + \sum_{j=0}^{2} \bar{K}_j \left(y_r^{(j)} - y^{(j)}(q, \dot{q}, v_2, \cdots, v_n) \right) \qquad (37)$$

for any choice of constant matrices $\bar{K}_j$ that renders the error equation exponentially stable: $e^{(3)} + \sum_{j=0}^{2} \bar{K}_j e^{(j)} = 0$, for $e := (y_r - y)$.

C. Example:Planar Three-Link Serial Structure Attached to a Pivot

This example treats the planar three-link robot depicted in Figure 5. The robot consists of three point masses connected by three rigid, massless links, with the links joined by an actuated revolute joint. The links are labelled L_1 through L_3 starting from the pivot and the masses are similarly labelled m_1 through m_3. The parameter values $L_1 = L_2 = 0.4, L_3 = 0.3, m_1 = 6.4, m_2 = 13.6, m_3 = 12$ were selected to approximate the biped robot RABBIT with the legs held together [3]. The objective is to demonstrate local exponential stability and asymptotic tracking about an equilibrium point.

1) **Mathematical representation:** The complete dynamic model is easily obtained using the method of Lagrange and yields immediately

$$\begin{array}{rcl} \dot{q}_0 &=& \frac{\sigma}{d_{0,0}} - \frac{d_{0,1}}{d_{0,0}}\dot{q}_1 - \frac{d_{0,2}}{d_{0,0}}\dot{q}_2 \\ \dot{\sigma} &=& -\frac{\partial V}{\partial q_0}(q) \\ \ddot{q}_1 &=& v_1 \\ \ddot{q}_2 &=& v_2, \end{array} \qquad (38)$$

where,

$a_{00} = (m_1 + m_2 + m_3)L_1^2 + (m_2 + m_3)L_2^2 + m_3 L_3^2$
$+2m_3 L_2 L_3 \cos(q_2)$
$a_{01} = 2(m_2 + m_3)L_1 L_2 + 2m_3 L_1 L_3 \cos(q_2)$
$a_{02} = -2m_3 L_1 L_3 \sin(q_2)$
$a_{10} = (m_2 + m_3)L_2^2 + m_3 L_3^2 + m_3 L_3^2 + 2m_3 L_2 L_3 \cos(q_2)$
$a_{11} = (m_2 + m_3)L_1 L_2 + m_3 L_1 L_3 \cos(q_2)$
$a_{12} = -m_3 L_1 L_3 \sin(q_2)$
$\frac{\partial V}{\partial q_0}(q) = -g_0(m_1 + m_2 + m_3)L_1 \cos(q_0)$
$-g_0(m_2 + m_3)L_2 \cos(q_0 + q_1) - g_0 m_3 L_3 \cos(q_0 + q_1 + q_2)$
$d_{0,0} = a_{00} + a_{01}\cos(q_1) + a_{02}\sin(q_1)$
$d_{0,1} = a_{10} + a_{11}\cos(q_1) + a_{12}\sin(q_1)$
$d_{0,2} = m_3 L_3(L_2 \cos(q_2) + L_1 \cos(q_1 + q_2))$.

2) **Control Law Design:** The key to applying the result is the explicit computation of the function p_1 in (28) used to define the outputs. Then for $q^* = 0$ and $-\pi < q_1 < \pi$, (28) can be evaluated explicitly as

$$p_1 = q_0 + \frac{c_1}{c_2} q_1 + \varphi_1 \circ \tan(\frac{q_1}{2}) + \varphi_2 \circ \tan(\frac{q_1}{2}), \qquad (39)$$

where,

$$\begin{array}{l} \varphi_1(x) = 2(\frac{a_{10}}{c_3} - \frac{a_{00}c_1}{c_2 c_3}) \arctan\left(\frac{(a_{00} - a_{01})x + a_{02}}{c_3}\right) \\ \varphi_2(x) = \frac{(a_{02}a_{11} - a_{01}a_{12})}{c_2} \ln\left(a_{00}(1 + x^2) + a_{01}(1 - x^2) + 2a_{02}x\right) \\ -\frac{a_{02}a_{11}}{c_2} \ln(1 + x^2) \\ c_1 = a_{01}a_{11} + a_{12}a_{02} \\ c_2 = a_{01}^2 + a_{02}^2 \\ c_3 = \sqrt{a_{00}^2 - a_{01}^2 - a_{02}^2}. \end{array} \qquad (40)$$

An equilibrium point $(q^e, 0)$ was found from $\frac{\partial V}{\partial q_0}(q)(q^e) = 0$: $q^e = (1.0472, 1.4522, -1.4522)$; see Figure 5 (a).

The control law design consists of the preliminary feedback (6) needed to place the system in form (10), the selection of two outputs, the dynamic extension, and a second static state feedback used to linearize and stabilize the input-output map. For the three-link robot, the outputs have been selected as

$$\begin{array}{rcl} y_1 &=& K(p_1 - p_1^e) + \sigma \\ y_2 &=& q_2 - q_2^e, \end{array} \qquad (41)$$

where $K > 0$ is to be chosen.

The dynamic extension is $\dot{v}_2 = \mu_2$, $v_1 = \mu_1$, which consists of adding a single integrator on v_2. The two outputs then have relative degree three with respect to μ, and the feedback controller is computed via (35) and (37). For the simulation, the matrices $\bar{K}_j$ were arbitrarily chosen to be diagonal and to place all of the eigenvalues of the error equation at -1. The free parameter in the output was arbitrarily chosen as $K = 5$. Since $d_{0,0}(q^e) \approx 14.5$, the zero dynamics is about one third as fast as the output error equation.

3) **Simulation results:** The simulation demonstrates asymptotic tracking and exponential stabilization. The initial condition was taken as $(1.1, 1.42, -1.80, 0, 0, 0)$, and is depicted in Figure 5 (b). For the first forty seconds, the robot is commanded to track sinusoidal references that cause it to execute a form of calisthenics, namely, deep knee bends; at forty seconds, the references are abruptly set to constant values corresponding to the equilibrium point q^e in order to demonstrate convergence to a constant set point. The asymptotic convergence of the outputs to the commanded references is shown in Figure 6. The evolution of the configuration

variables and the applied joint torques is shown in Figure 7. An animation of the motion is available at [8].

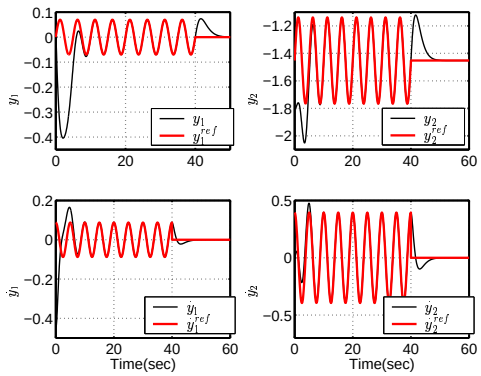

Fig. 6. Demonstration of asymptotic tracking and stabilization for the three-link mechanism. For the first forty seconds, the motion consists of an initial transient, followed by tracking of sinusoidal trajectories that correspond to knee bends. At forty seconds, the reference trajectory is abruptly set to zero, thereby commanding the system to an equilibrium point.

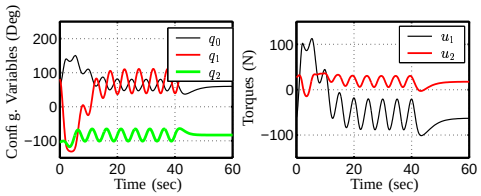

Fig. 7. Demonstration of asymptotic tracking and stabilization for the three-link mechanism; see Figure 6 for details. The plots show the configuration variables (left), joint torques (right).

VI. Conclusions

Two novel control results have been presented. When the generalized momentum conjugate to the cyclic variable was not conserved, conditions were found for the existence of a set of outputs that yielded a one-dimensional, exponentially stable zero dynamics. A controller that achieves asymptotic stabilization and tracking is then easily constructed. When the generalized momentum conjugate to the cyclic variable was conserved, a reduced system was constructed and conditions were found for the existence of a set of outputs that yielded an empty zero dynamics. A change of coordinates and controller that achieve input to state linearization are then easily constructed. The solutions to these two control problems had a common underlying element: the computation of a function of the configuration variables that had relative degree three with respect to one of the input components after an appropriate state feedback. It was interesting that this function arose by partially integrating a physical quantity, the conjugate momentum. The theoretical results were illustrated on two simple examples.

Acknowledgments

The work of J.W. Grizzle was supported by NSF grant ECS-0322395.

References

[1] F. Bullo and K. M. Lynch. Kinematic controllability for decoupled trajectory planning in underactuated mechanical systems. *IEEE Transactions on Robotics and Automation*, 17(4):402–412, August 2001.

[2] L. Cambrini, C. Chevallereau, C.H. Moog, and R. Stojic. Stable trajectory tracking for biped robots. In IEEE Press, editor, *Proceedings of the 39th IEEE Conference on Decision and Control, Sydney, Australia*, pages 4815 –4820, December 2000.

[3] C. Chevallereau, G. Abba, Y. Aoustin, E.R. Plestan, F. Westervelt, C. Canduas-de Wit, and J.W. Grizzle. Rabbit: A testbed for advanced control theory. *IEEE Control Systems Magazine*, To appear in October 2003. see [8] for a copy.

[4] C. Chevallereau and Aoustin. Optimal reference trajectories for walking and running of a biped robot. *Robotica*, 19(5):557–569, September 2001.

[5] M. Fliess, J. Levine, P. Martin, and P. Rouchon. A lie-backlund approach to equivalence and flatness of nonlinear systems. *IEEE Transactions on Automatic Control*, 44(5):922 –937, May 1999.

[6] T. Geng and X. Xu. Flip gait synthesis of a biped based on poincare map. In *Proc. of the Second International Workshop On Robot Motion And Control, Bukowy Dworek, Poland*, pages 239–243. IEEE Robotics and Automation Society, October 2001.

[7] H. Goldstein. *Classical Mechanics*. Addison Wesley, second edition, 1980.

[8] J.W. Grizzle. Publications on robotics and control. *http://www.eecs.umich.edu/∼grizzle/papers/robotics.html*, September 2003.

[9] J.W. Grizzle, C.H. Moog, and C. Chevallereau. Nonlinear control of mechanical systems with one degree of underactuation. *submitted to IEEE Trans. on Automatic Control*, 2003. See [8] for a preprint.

[10] A. Isidori. *Nonlinear Control Systems: An Introduction*. Springer-Verlag, Berlin, third edition, 1995.

[11] I. Kolmanovsky, N.H. McClamroch, and V.T. Coppola. New results on control of multibody systems which conserve angular momentum. *Journal of Dynamical and Control Systems*, 1(4):447–462, 1995.

[12] M. Miyazaki, M. Sampei, and M. Koga. Control of a motion of an acrobot approaching a horizontal bar. *Advanced Robotics*, 15(4):467–480, 2001.

[13] J. Nakanishi, T. Fukuda, and D.E. Koditschek. A brachiating robot controller. *IEEE Transactions on Robotics and Automation*, 16(2):109–123, April 2000.

[14] R. Olfati-Saber. Control of underactuated mechanical systems with two degrees of freedom and symmetry. In *Proc. of the American Control Conference at Chicago, IL*, pages 4092–4096, June 2000.

[15] R. Ortega, M.W. Spong, and F. Gomez-Estern. Stabilization of underactuated mechanical systems via interconnection and damping assignment. *IEEE Transactions on Automatic Control*, 47(8):1281–1233, August 2002.

[16] M. Raibert. *Legged robots that balance*. MIT Press, Mass., 1986.

[17] M. Rathiman and R. Murray. Configuration flatness of lagrangien systems underactuated by one control. *SIAM J. Control and Optimization*, 36(1):164–179, 1998.

[18] P. Rouchon, M. Fliess, J. Levine, and P. Martin. Flatness, motion planning and trailer systems. In *Proceedings of the 32nd IEEE Conference on Decision and Control*, pages 2700 –2705. IEEE, December 1993.

[19] M. Sampei, H. Kiyota, and M. Ishikawa. Control strategies for mechanical systems with various constraints—control of nonholonomic systems. In *IEEE Conf. on Systems, Man, and Cybernetics, III*, pages 158–167, 1999.

[20] D. Seto and J. Baillieul. Control problems in super-articulated mechanical systems. *IEEE Transactions on Automatic Control*, 39(12):2442 –2453, December 1994.

[21] M.W. Spong. The swing up control problem for the acrobot. *IEEE Control Systems Magazine*, 15(1):49–55, February 1995.

[22] E. Westervelt, J.W. Grizzle, and D.E. Koditschek. Hybrid zero dynamics of planar biped walkers. *IEEE Transactions on Automatic Control*, 48(1):42–56, January 2003.

[23] M. Yamakita, T. Yonemura, Y. Michitsuji, and Z. Luo. Stabilization of acrobot in upright position on a horizontal bar. In *Proc. of the IEEE International Conference on Robotics and Automation, Washington, DC*, pages 3093–3098, May 2002.